Available online at www.sciencedirect.com
SCIENCE DIRECT®
International Journal of Heat and Mass Transfer 47 (2004) 489–500
International Journal of HEAT and MASS TRANSFER
www.elsevier.com/locate/ijhmt

Heat transfer and wall pressure characteristics of a twin premixed butane/air flame jets

L.L. Dong, C.W. Leung *, C.S. Cheung

Department of Mechanical Engineering, The Hong Kong Polytechnic University, Hung Hom, Kowloon, Hong Kong

Received 20 February 2003; received in revised form 12 July 2003

Abstract

Experimental studies were carried out to investigate the flame shape and the heat transfer and wall pressure characteristics of a pair of laminar premixed butane/air flame jets impinging vertically upon a horizontal water-cooled flat plate at jet Reynolds numbers of 800, 1000 and 1200, respectively. Equivalence ratio of the butane/air mixture was maintained constantly at unity. The flame shape, the pressure distribution on the impingement plate and the heat transfer from the flame to the plate were greatly influenced by the interference occurred between the two flame jets. This interference caused a sharp pressure peak at the between-jet midpoint and the positive pressures at the between-jet area, which led to the separation of the wall jet from the impingement plate after collision. Such interference became more significant when the non-dimensional jet-to-jet spacing (S/d) and the nozzle-to-plate distance (H/d) were reduced. Heat transfer in the interaction zone between the jets was at the lowest rate due to this interference at the smallest S/d ratio of 2.6, resulting from the separation of the high-temperature inner reaction zone of the flame from the impingement plate. On the other hand, the interference enhanced the heat transfer in the interaction zone between the jets when the S/d ratio was greater than 5, by enhancing the heat transfer coefficient. The average heat flux of the impingement plate was found to increase significantly with the increasing H/d ratio until $H/d = 6$. The present study provided detailed information on flame shape and the heat transfer and wall pressure characteristics of a twin laminar pre-mixed impinging circular flame jets, which has rarely been reported in previous studies.

Keywords: Butane/air premixed combustion; Twin impinging flame jets; Heat transfer and wall pressure

1. Introduction

Impinging jets have been widely used in heating, cooling and drying processes for their excellent heat transfer performance. Both single and multiple jets are used for different purposes. A single jet is usually employed to produce localized heating or cooling [1,2]. In many applications, a large surface area is required to be heated or cooled, or enhancement of global heat transfer is needed, such as in water heaters, domestic gas stoves and the thrust-augmenting ejectors for VTOL/STOL aircraft, thus, it is necessary to apply multiple-jet system [1–4]. Using information for a single jet to design a multiple-jet system is usually not valid, because of the strong interaction between the jets, except when the jets are widely spaced, so that no interaction can be reasonably assumed [5]. Therefore, the effects of the interaction between the jets on the flow field and the heat transfer characteristics for a multiple-jet system should be studied to fill the gap.

Many previous studies dealt experimentally and numerically with multiple impinging turbulent air jets [6–13]. Martin [14] and Polat et al. [15] reviewed the heat transfer characteristics of multiple impinging air jets. Koopman and Sparrow [1] concluded that the basic difference in the fluid mechanics of single and multiple jets was the two types of interaction between the jets in the multiple-jets system. The first type was the interference between adjacent jets prior to impingement on the

* Corresponding author. Tel.: +852-2766-6651; fax: +852-2365-4703.
E-mail address: mmcwl@polyu.edu.hk (C.W. Leung).

0017-9310/$ - see front matter © 2003 Elsevier Ltd. All rights reserved.
doi:10.1016/j.ijheatmasstransfer.2003.07.019

Nomenclature

d	nozzle exit diameter (m)
H	distance between the nozzle and the impingement plate (m)
Nu	Nusselt number ($= \alpha d/\lambda$)
P	differential wall pressure (Pa) ($= P_w - P_\infty$)
P_w	pressure of the impinging jet on the wall (Pa)
P_∞	atmospheric pressure (Pa)
$\dot{q}$	heat flux on the impingement plate (W/m^2)
$\bar{q}$	average heat flux on the impingement plate (W/m^2)
r	radial distance from the midpoint between the two nozzles (m)
Re	jet Reynolds number ($= u_{out} d/v$)
S	distance between the centers of the two nozzles (m)
u	velocity of butane/air mixture (m/s)
x	central streamline (m)
y	central span-wise line (m)
α	heat transfer coefficient (W/m^2 K)
λ	thermal conductivity (W/m K)
v	kinematic viscosity (m^2/s)
ϕ	equivalence ratio of butane/air mixture [= (stoichiometric butane/air volume ratio)/(actual butane/air volume ratio)]

Subscript

out	at the nozzle exit

surface. The second type was the collision of the two wall jets, which were generated after impingement. Such collision became significantly important when the jets were closely spaced, the nozzle-to-plate distance was small, and the jet velocity was high. Kind and Suthanthiran [16] performed an experimental study on the interaction produced by the collision of two diametrically opposed turbulent wall jets. They found that the separation processes due to collision were dynamically similar. It could be explained by the "frozen-flow" concept suggested by Stratford [17] and Townsend [18]. Baydar [19] and Huber [20] showed the occurrence of a secondary stagnation region where the wall jets of the adjacent jets were meeting and colliding with each other, resulting in an increase of local pressure and a separation of the fluid from the surface.

Koopman [21] revealed high heat transfer coefficients for multiple jets in the stagnation region and at the second stagnation point (i.e., the midpoint between the two neighboring jets). Carcasci [22] investigated a row of turbulent air jets impinging downward on a surface with flow-visualization techniques and found two types of vortex. The first type was a large main vortex produced by the flow turning upward after the wall jets collided with each other. The other type consisted of two lower adverse vortices formed between the main vortex and the impingement plate, which were generated by the interaction of the two main vortices. When the jets were impinging downward on the surface, the up swelling of spent flow formed by the collision of the jets was identified as a fountain up-wash flow by many investigators [23–26]. It was found that this up-wash flow was characterized by high turbulence. Tanaka [27,28] found that a particular feature of the two-dimensional parallel flow of a twin jets was the appearance of a sub-atmospheric region between the jets, owing to the entrainment of the fluid by the turbulent jet. Consequently, the two jets attracted each other and finally combined together. Mikhail et al. [29] found that the average Nusselt number of the twin jets system increased with decreasing S/d. This increase was due to the coverage of more impingement surface area by the stagnation region where a maximum local heat transfer ensued. This suggestion was further confirmed by Obot and Trabold [30]. However, according to Huber [20], the effect of interaction of adjacent jets was to reduce the local heat transfer rate if the jet-to-jet spacing became too small and/or the jet diameters were too large. Heat transfer equations for multiple turbulent impinging air jets were provided by several investigators for the calculation of both local and average Nusselt numbers [14,20].

Compared to the numerous investigations on multiple impinging air jets, very few has been done with flame jets of similar configuration. Most previous investigations on impinging flame jets concentrated on a single jet [31–38]. The available information on multiple impinging flame jets was related to the study of radial jet reattachment flames and the multi-jets used in the rapid heating furnace. Malikov et al. [39] studied the heat transfer in a rapid heating furnace with a multi-jet combustion chamber. Mohr et al. [40] investigated the thermal performance of radial jet reattachment flames with a pair of flame jets, while the heat transfer characteristics of radial jet reattachment flames with three flame jets was studied by Wu et al. [41]. However, information about impinging flame jets emitted from multiple in-line nozzles is so far unavailable, although they are used in many applications such as domestic gas appliances. Viskanta [42,43] recommended that understanding of the flame structure and heat transfer

characteristics of impinging multiple flame jets should be a priority for future research in this area.

The present study, performing with a pair of laminar pre-mixed butane/air flame jets, is an extended study of the previous investigations [44,45]. Experiments were performed to investigate the flame shape, the heat transfer and wall pressure characteristics of a twin impinging flame jets. Photographs of free/impinging flames were presented to facilitate flame shape visualization. The effects of the jet-to-jet spacing (S/d) and the nozzle-to-plate distance (H/d) and the jet Reynolds number (Re) were examined.

2. Experimental setup and method

The flame jet impingement system was composed of two parts: the heat generation system and the heat absorption system, as shown schematically in Fig. 1.

2.1. Heat generation system

The flame holders were two identical brass tubes and each of them had a length of 50 mm and an inner diameter of 5 mm. Metered butane and compressed air were premixed in a brass cylinder, before entering the cylindrical aluminum equalization chamber via a 200 mm long stainless steel tube. The equalization chamber was filled with stainless steel beads to produce uniform flow and prevent the flame from flashing back. The butane/air mixture then entered the flame holder with unity equivalence ratio and was ignited and stabilized at the tube rims. The internal surfaces of the brass tubes were polished to facilitate a smooth velocity profile at the exit. The three-dimensional positioner enabled each of the attached burners to be fixed at a desired position relative to the impingement surface.

2.2. Heat absorption system

The flame impingement surface was a square copper plate of 200 mm long, 200 mm wide and 8 mm thick. It was uniformly cooled on its backside by a cooling water jacket. Copper was selected to fabricate the plate because of its excellent thermal conductivity. The top plate of the cooling water jacket was made of plexiglass to enable the water flow to be visualized. A stainless steel frame was used to support the copper plate and the cooling water jacket, so that the plate could be placed either horizontally or tilted at a selected angle relative to the burner. After a change in the operating condition had been made, measurements were only conducted after the steady-state conditions had been established again.

2.3. Measurement of wall pressure, heat flux and flame shape

A single pressure tap of 1 mm diameter was drilled through the copper plate at its center. The radial pressure distributions along the plate were obtained by moving the three-dimensional burner positioner in the x-, y- and z-directions, while the plate remained stationary. The pressure tap was connected via a flexible

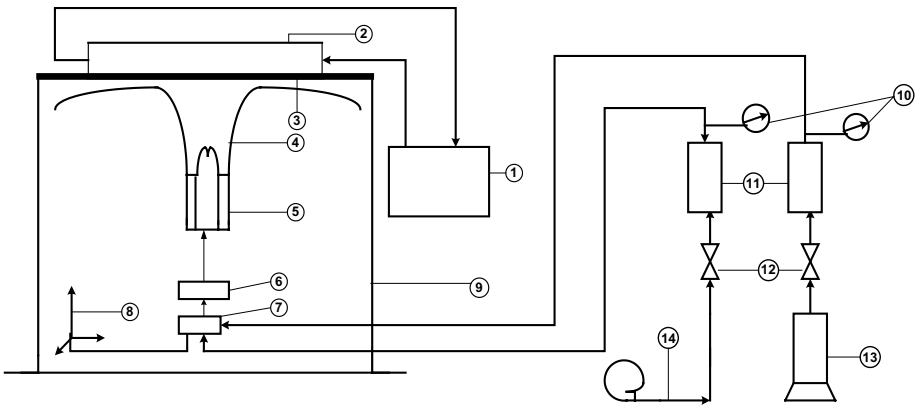

1. Thermostat
2. Cooling Water Jacket
3. Impingement Plate
4. Flame Jet
5. Nozzle
6. Equilizating Chamber
7. Premixed Chamber
8. 3-D Positioner
9. Angle Steel Holder
10. Pressure Gauge
11. Flow Meter
12. Valve
13. Fuel Tank
14. Compressed Air Line

Fig. 1. Schematic of the experimental setup.

tube to an inclined differential manometer with an accuracy of ±2% of the full scale.

The local heat flux from the flame to the plate was measured with a ceramic heat flux transducer having a very small effective sensing area of 3 mm × 3 mm. It was attached directly to the copper plate. The heat flux distributions in the x- and y-directions were measured by moving the three-dimensional burner positioner as mentioned previously. A PC-acquisitor was used to record the heat flux. Data reported here were the average values of the data obtained consecutively in 30 s at a rate of 500 samples/s.

Photographs of the flame shapes at different experimental conditions were taken with a digital camera.

Experiments were carried out to study the influences of S/d, H/d and Re on the flame shape and the heat transfer and wall pressure characteristics of a twin laminar premixed butane/air impinging flame jets. The S/d ratio was selected from 2.6 to 10 to cover small, moderate and large jet-to-jet spacing. The H/d ratio varied from 1 to 7 to include partly or entirely the inner cone length of the flame. The Re was chosen to be 800, 1000 and 1200 to ensure a laminar flow condition. All the tests were performed at a unity equivalence ratio.

3. Error analysis

The coordinate system used in the present study is shown in Fig. 2. An error analysis was performed using the methods proposed by Kline and McClintock [46]. The maximum and minimum uncertainties for the experimentally measured local heat fluxes were 13% and 3.6%, respectively.

To ensure repeatability of the results, three runs with identical operating conditions were conducted and their results were then averaged. The minimum and maximum standard deviations in the highest heat flux values were 1.2% and 14.7%, respectively of their mean values.

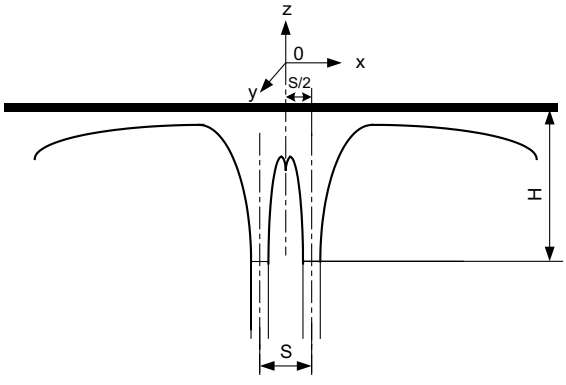

Fig. 2. Coordinate system of the impingement plate.

4. Results and discussions

The pressure and heat flux distributions on the impingement plate, as well as the flame shapes were obtained for laminar flames with Reynolds numbers maintaining at 800, 1000 and 1200, respectively. Effects of Re, H/d, and S/d on the flame shape and the heat transfer and wall pressure characteristics of the twin premixed butane/air impinging flame jets were fully examined. The equivalence ratio was maintained at unity throughout the present study.

4.1. Flame shape

Photographs of both free flame jets and impinging flame jets at $Re = 1200$, with a jet-to-jet spacing of $2.6d$ or $6d$, under a nozzle-to-plate distance of $2d$ or $6d$ are shown in Figs. 3 and 4. It was found that all the flames under investigation appeared to be laminar, and each of them had a thin turquoise-blue inner cone and a thin light-blue outer layer, however, the impinging flame jets exhibited different shapes when S/d or H/d was changed.

The flames produced with a small S/d ratio of 2.6 are shown in Fig. 3. It was found from Fig. 3(a) that the free flame jets were clearly separated around the nozzle exits. Away from this region, the outer layers merged to appear as a single jet at the interacting side, which indicated the occurrence of the before-impingement interaction as suggested by Koopman and Sparrow [1] for the multiple air jets. When the flame jets impinged on the plate with a small nozzle-to-plate distance of $H/d = 2$, a strong jet-to-jet interference was observed from Fig. 3(b). The flames were significantly altered at the interacting side, with their inner cone layers collided with each other at the middle plane between the two nozzles. After impinging on the plate, they were separated from the plate and forced to turn downward. It could be inferred from this alteration of flow field that the wall pressure in the interaction region was greater than the ambient pressure. This separation of the flame from the impingement surface had also been found for adjacent isothermal air jets [1,20,30]. The wall jet was thought to encounter an adverse pressure gradient along the wall as it was entering into the interaction region, and thus caused the boundary layer to separate from the impingement plate. As a result, separation bubbles were formed in this region. These bubbles were also found by Carcasci [22] and Huber [20], and were referred to as vortices. Mikhail et al. [29] and Baydar [19] also suggested the similar flow pattern. The shape of the impinging flame jets at a larger nozzle-to-plate distance of $H/d = 6$, is shown in Fig. 3(c). The interference of the two inner cone layers was not so clearly observed, which indicated that the pressure gradient at the interacting zone was lower than that obtained at $H/d = 2$, due to the weaker between-jet interaction.

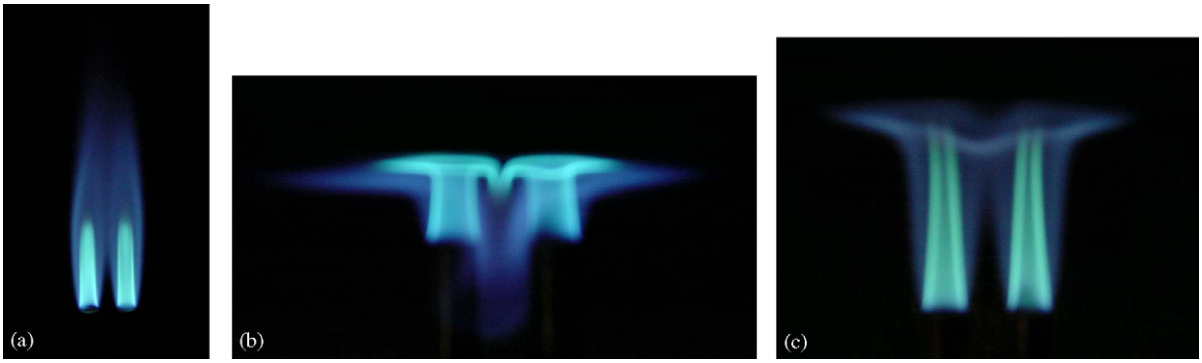

Fig. 3. (a) Photograph of a pair of free flame jets viewed in the x-plane ($Re = 1200$; $S/d = 2.6$; $\phi = 1$). (b) Photograph of a pair of impinging flame jets viewed in the x-plane ($Re = 1200$; $S/d = 2.6$; $H/d = 2$; $\phi = 1$). (c) Photograph of a pair of impinging flame jets viewed in the x-plane ($Re = 1200$; $S/d = 2.6$; $H/d = 6$; $\phi = 1$).

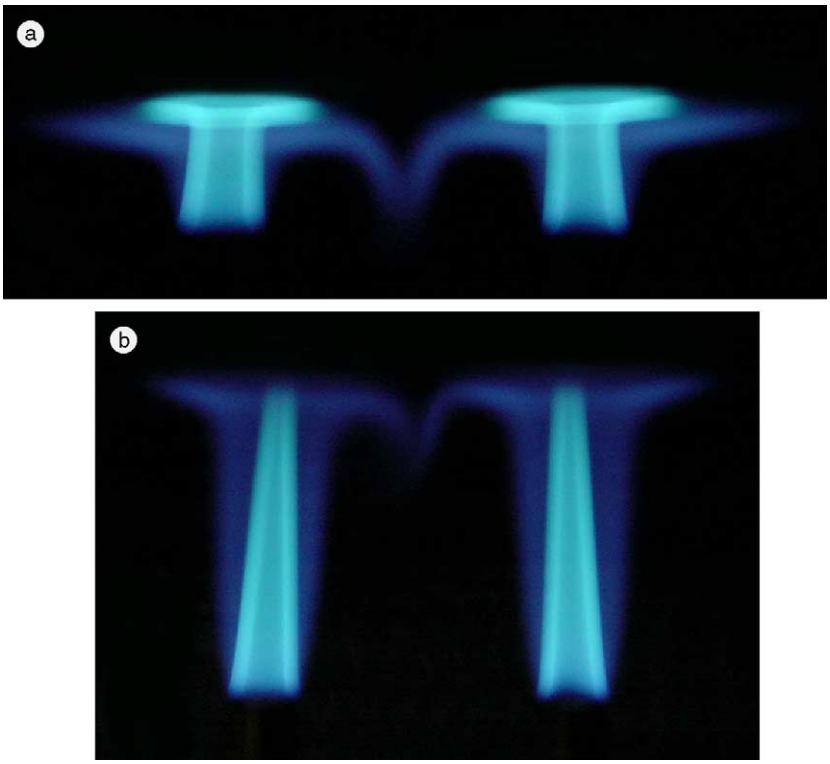

Fig. 4. (a) Photograph of a pair of impinging flame jets viewed in the x-plane ($Re = 1200$; $S/d = 6$; $H/d = 2$; $\phi = 1$). (b) Photograph of a pair of impinging flame jets viewed in the x-plane ($Re = 1200$; $S/d = 6$; $H/d = 6$; $\phi = 1$).

When the S/d ratio was increased to 6, no interaction between the two free flame jets could be observed. Thus, Fig. 4 only presents the photographs of impinging flame jets. It was noted from Fig. 4(a) that at the small nozzle-to-plate distance of $H/d = 2$, the two inner layers did not interfere with each other. However, the outer flame layers collided at the middle plane on the interacting side and then forced to turn downward. The between-jet interference became weaker when the S/d ratio was increased from 2.6 to 6. It was noted that the thickness of the downward flame decreased as it was moving away from the impingement plate, as shown in Fig. 4(a). This was rather different from the finding of Saripalli [47] obtained from a pair of downward impinging water jets, where thickness of the upward flow after collision, called a "fountain up-wash flow", increased as it moved away

from the impingement surface. This difference should be due to the buoyancy effect of the hot combustion gas in the present study. Combination of the downward force caused by the pressure gradient in the interacting zone and the upward force due to the buoyancy effect resulted in the progressive reduction of thickness of the interacting flame after impingement. The photograph of the flame jets at the larger nozzle-to-plate distance of $H/d = 6$, is shown in Fig. 4(b). A slightly downward flow of the outer flame layers was observed indicating that the interference between the two adjacent flame jets reduced with increasing H/d ratio.

If the S/d ratio was further increased to 10, no evident collision of the two flame jets was found for both the free and the impinging jets operating under the small and large H/d ratios of 2 and 6. The influence of the interference between the jets on the shape of the flame could no longer be observed, and the two flame jets appeared to be two isolated single jets. For simplicity, their photographs were not provided here. It can be concluded that the interference between the jets of the multiple flame jets system increased with reducing S/d or H/d ratio.

4.2. Impingement surface pressure distribution

The variation of the local pressure on the surface impinged by the flame jets was measured to help understanding the flame shape and the local heat transfer characteristics. The pressure distributions on the impingement surface at a Reynolds number of 1200 obtained under small and large H/d ratios of 2 and 6 are shown in Fig. 5(a)–(c). Considering the symmetrical condition at both sides of $x = 0$, the plots are presented from the midpoint between the jets (i.e., $x = 0$) to one edge of the plate.

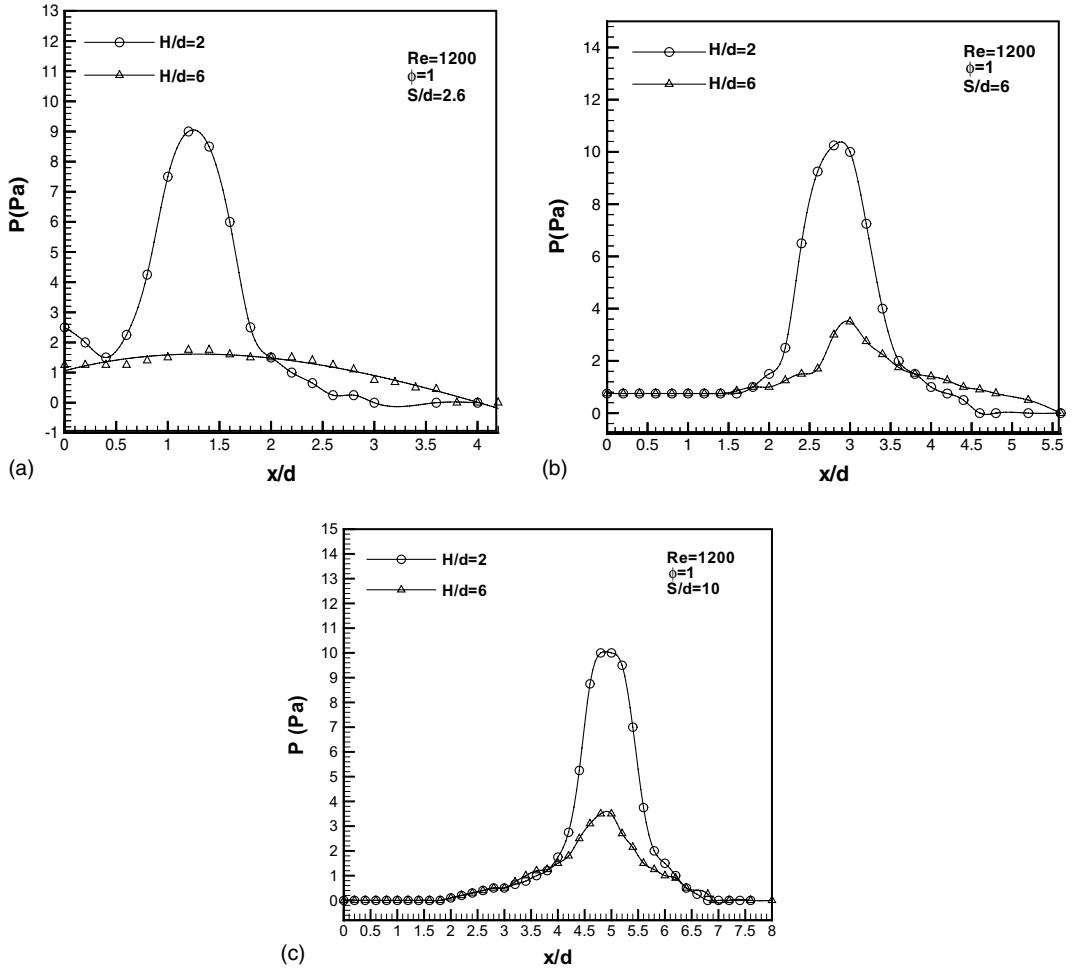

Fig. 5. (a) Wall pressure distribution at $S/d = 2.6$. (b) Wall pressure distribution at $S/d = 6$. (c) Wall pressure distribution at $S/d = 10$.

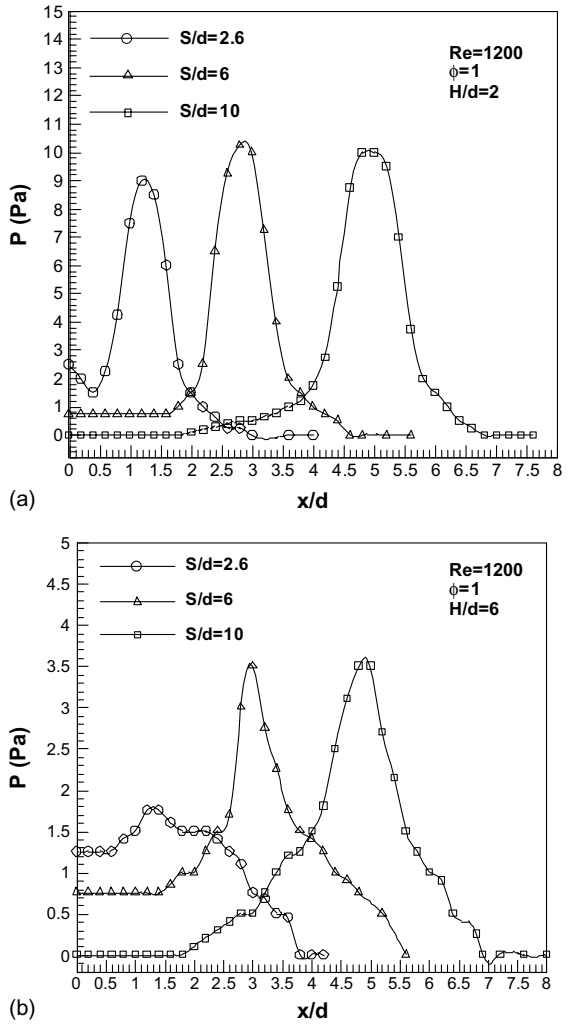

Fig. 6. (a) Effects of S/d on the wall pressure distribution at $H/d = 2$. (b) Effects of S/d on the wall pressure distribution at $H/d = 6$.

It was observed from Fig. 5(a) that under small S/d and H/d ratios of 2.6 and 2, there were two pressure peaks occurred. In addition to the one at the stagnation point of the impinging flame jet, another pressure peak occurred at the midpoint of the two jets (i.e., $x = 0$). Thus, an adverse pressure gradient was encountered when the wall jets were spreading radially, as found from the study of impinging air jets by Obot and Trabold [30]. As a result, a separation of the wall jet from the impingement plate occurred, as shown in Fig. 3(b). The second pressure peak (i.e., at $x = 0$) was not observed when either the S/d or H/d ratio was increased, which reduced the between-jet interference. This was also reflected in Figs. 3(c) and 4(b) that no flame jet separation from the impingement plate was found.

It was also shown in Fig. 5 that at $H/d = 6$, the wall pressure distribution was much more uniform and the wall pressures within the impingement region were much lower than those obtained at $H/d = 2$. At a small H/d ratio of 2, the nozzle-to-plate distance was smaller than the inner core length, hence, some unreacted butane/air mixture impinged directly on the plate with the nozzle exit velocity. However, when the H/d ratio was increased to 6, the impinging velocity at the vertical axis of the jet close to the plate decreased dramatically due to the transfer of momentum to the entrained air and the chemical-reaction-induced gas expansion.

The information presented in Fig. 5(a)–(c) was rearranged in Fig. 6 to illustrate clearly the effect of S/d ratio on the wall pressure. It could be found from Fig. 6 that positive pressure areas occurred between the two adjacent jets under small and moderate S/d ratios of 2.6 and 6. This positive pressure increased with decreasing S/d and H/d ratios, as shown in Fig. 5(a), due to the increased between-jet interference. This positive pressure differential also led to the downward flow of the wall jets on the interacting side.

4.3. Heat transfer characteristics

The interference between the two adjacent jets has been suggested to have significant influence on the heat transfer of a multiple impinging jets system [21,48]. Thus, the effects of the H/d and S/d ratios, which can affect the between-jet interference significantly, on both the local and average heat transfer rates, are discussed.

4.3.1. Local heat transfer distribution

4.3.1.1. Effects of S/d ratio. The heat flux distributions on the impingement plate obtained at different S/d and H/d ratios are shown in Fig. 7, at a H/d ratio of 6 and a Reynolds number of 1200. The local heat flux distributions for half of the plate (i.e., from the midpoint at $x = 0$ to one edge of the plate) when the S/d ratio is increased from 2.6 to 10, are shown in Fig. 8. The results presented in Fig. 8 were obtained at a H/d ratio of 2 and a Reynolds number of 1000.

It was observed from Fig. 7(a) that the heat flux contours exhibited were almost two semi-circles separated by the line at $x = 0$, with a low heat flux zone around the midpoint between the two flame jets for $S/d = 2.6$. The occurrence of this cool central zone indicated that the interference between the two flame jets was to suppress their heat transfer to the plate. It was resulted from the separation of the high temperature combustion gas from the impingement plate.

When the S/d ratio was increased to 6, the heat flux distribution as shown in Fig. 7(b) almost appeared to be those produced by two separate jets, except that some interaction was observed where the two wall jets collided with each other. This was due to the reduced interaction

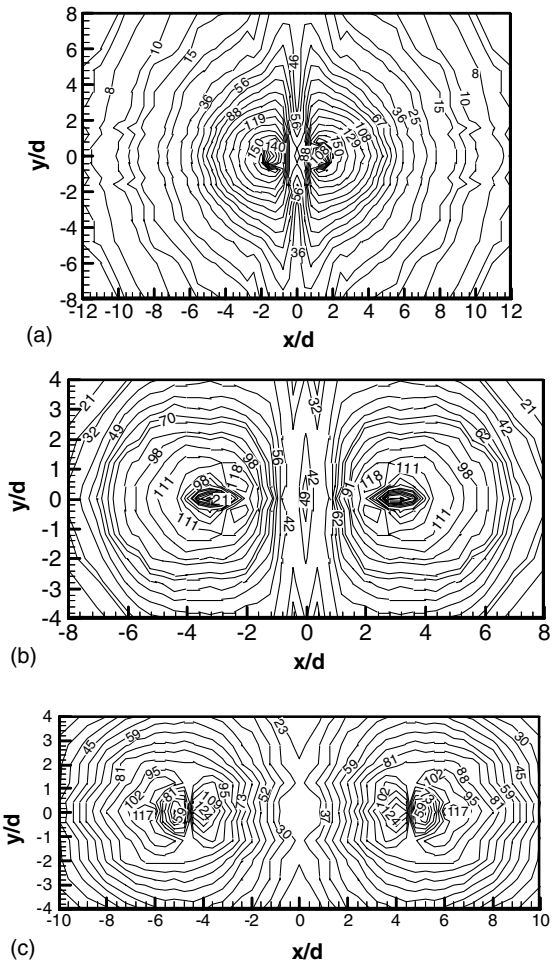

Fig. 7. (a) Heat flux contour at $Re = 1200$, $H/d = 6$, $S/d = 2.6$, $\phi = 1$. (b) Heat flux contour at $Re = 1200$, $H/d = 6$, $S/d = 6$, $\phi = 1$, (c) Heat flux contour at $Re = 1200$, $H/d = 6$, $S/d = 10$, $\phi = 1$.

between the two jets when the S/d ratio was increased. It could also be observed that in the interacting zone, the heat flux gradient was larger on the x-axis than on the y-axis, which was resulted from the different flow patterns in these two directions. The outer flame layer on the interacting side was longer in the y-direction due to the spreading of the combined jets in that direction after collision. Thus a longer distance in the y-direction was covered by this outer flame layer, which led to a more uniform heat flux distribution in this direction.

When the S/d ratio was further increased to 10, no increase in heat flux in the interaction zone was found in contrast to the case of $S/d = 6$, as shown in Fig. 7(c). It showed that with a large S/d ratio, the heat transfer characteristics of a pair of impinging flame jets were similar to those of two isolated jets.

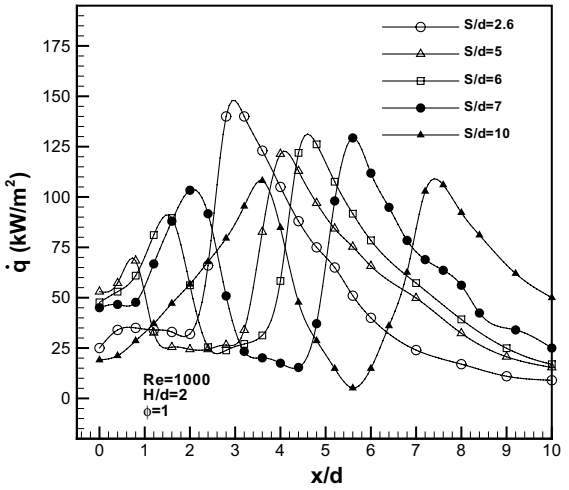

Fig. 8. Effect of S/d on heat flux distribution from flame to the plate along x-axis under $y = 0$.

Since the interference between the two jets occurred essentially in the x-direction rather than the y-direction, comparison of the effect of varying the S/d ratio on the heat flux distribution along the x-axis is only shown in Fig. 8. It was observed that all the curves, except the one at $S/d = 2.6$, exhibited two obvious peaks. At $S/d = 2.6$, only one peak was found on the non-interacting side. This was due to the separation of the inner reaction zone from the impingement plate, as shown in Fig. 3(b). The small jet-to-jet spacing led to the connection of the cool central core regions of the two impinging flame jets, which contained unburned butane/air mixture, in the interacting region. The unburned mixture contacted the impingement plate due to the separation of the reaction zone, resulting in a relatively big cool central zone with rather low heat flux. This was significantly different from the heat transfer characteristics of the impinging air jets, where the heat transfer on the interacting side was found to enhance because of the strong interference between the jets, as verified by Koopman [21].

Between the S/d ratios of 5 and 7, the first heat-flux peak increased when the S/d ratio was increased, indicating a reduced inhibition of the collision to complete combustion. When the S/d ratio was increased, there was more radial distance along the impingement plate for the flame jet to burn completely after impingement, so that the peak heat flux in the interacting zone increased accordingly. In addition, the second heat flux peaks on the non-interacting side were similar to each other for the S/d ratios of 5, 6 and 7. Apart from this, the value of the second heat-flux peak increased with decreasing S/d ratio. The highest value occurred at $S/d = 2.6$, while the lowest value was located at $S/d = 10$. Considering that the heat transfer performance of the twin-jet system at $S/d = 10$ was similar to those of

two isolated impinging jets as stated previously, it could be concluded that the second heat-flux peak on the non-interacting side was enhanced by the interference between the jets. This was due to the turbulence induced by mixing, which was caused by collision of the jets in the interacting zone, penetrating further toward the non-interacting sides of the individual jets, as suggested by Goldstein and Timmers [49], to enhance the second heat-flux peak.

4.3.1.2. Effects of Reynolds number. The effects of Reynolds number on heat transfer rates at a S/d ratio of 2.6 and a H/d ratio of 6 is shown in Fig. 9. It was found that the heat transfer rate was enhanced with increasing Reynolds number due to the increased convective heat transfer, as in the case for the single impinging flame jet [31–35]. Koopman [21] investigated the effect of Re on a pair of cold air jets and found that the heat transfer coefficients at the midway position were enhanced by a higher jet Reynolds number, which contributed to the enhancement of heat flux at the midpoint. It was found from Fig. 9 that the heat transfer distribution curves were similar for different Reynolds numbers of 800, 1000 and 1200. All the three curves exhibited two peaks, with the second peak being higher than the first one. It was also found that the influence of *Re* on heat flux was evident only within $x/d < 5.6$. The heat flux values were almost the same beyond this position.

4.3.1.3. Effects of H/d ratio. The effects on heat flux distributions on the impingement plate of varying the H/d ratio from 1 to 7 at a S/d ratio of 2.6 and a Reynolds number of 1200 were investigated. It was observed from Fig. 10 that the influence of the H/d ratio on the heat flux distributions was only significant within the region of $x/d \leqslant 4$. Beyond this region, only a trivial difference between the heat flux obtained at different H/d ratios was found. For all the H/d ratios investigated from 1 to 7, it was found that the heat flux at the midpoint between the two jets exhibited a very low value. This was due to the separation of the high temperature reaction zone from the impingement plate, as stated previously. It could also be observed that when the H/d ratio was $\leqslant 6$, the heat flux increased with increasing H/d ratio in the region of $x/d \leqslant 4$. This was because, the smaller the nozzle-to-plate distance, the stronger the interference between the two jets in the interaction zone. The stronger interference promoted the separation of the high temperature reaction zone away from the impingement plate, and hence reduced the heat flux. When the H/d ratio was increased to 7, a decrease in the heat flux was found. When the H/d ratio reached 7, the nozzle-to-plate distance exceeded the length of the inner cone where reaction occurred. Thus, the relatively cooler outer layer of the flame came into contact with the impingement plate, resulting in a decreased heat flux. It was also observed from Fig. 10 that the heat flux distribution curves were similar for the smaller H/d ratios of 1 and 2, which exhibited only one peak in the non-interacting side, while two heat-flux peaks were found for the cases with larger H/d ratios. Plateaus with rather low heat flux were found when $x/d < 2$ for the H/d ratios of 1 and 2. These plateaus resulted from the separation of the inner reaction zone from the impingement plate. When the H/d ratio exceeded 3, no separation of the inner cone layer from the impingement plate was observed.

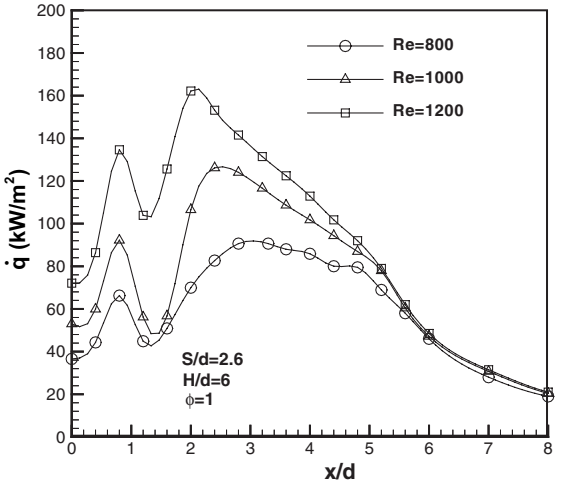

Fig. 9. Effect of *Re* on heat flux distribution from flame to the plate along x-axis under $y = 0$.

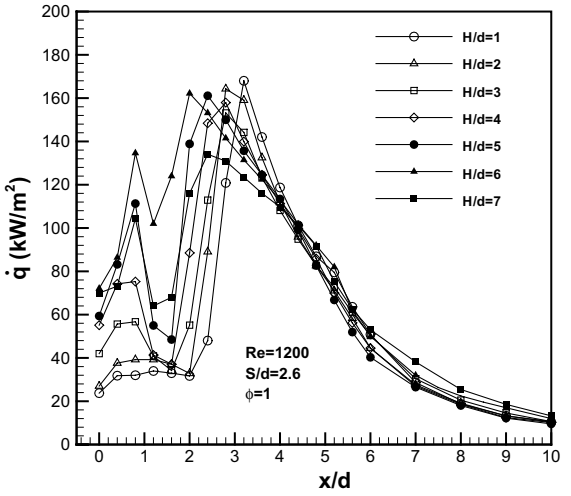

Fig. 10. Effect of H/d on heat flux distribution from flame to the plate along x-axis under $y = 0$.

4.3.2. Average heat flux distribution

In many applications, the average heat flux is an important factor when evaluating the thermal performance of a heating or cooling system. The average heat flux

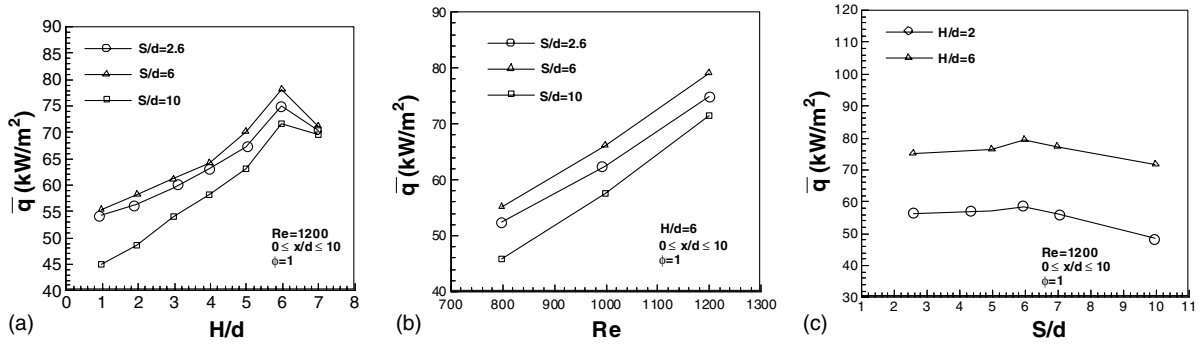

Fig. 11. (a) Effect of H/d on the average heat flux along x-axis under $y = 0$. (b) Effect of Re on the average heat flux along x-axis under $y = 0$. (c) Effect of S/d on the average heat flux along x-axis under $y = 0$.

distributions along the x-axis of the impingement plate were obtained by the trapesoidal method. The effects of H/d ratio, Re and S/d ratio on the average heat flux distributions are shown in Fig. 11. It was observed from Fig. 11(a) that for all the S/d ratios of 2.6, 6 and 10, the average heat flux increased with increasing H/d ratio until the maximum was obtained at $H/d = 6$, at a Reynolds number of 1200. After that the average heat flux began to decrease. This phenomenon followed the variation in local heat flux distributions as shown in Fig. 10. It was also found that the highest average heat flux occurred at the S/d ratio of 6, and the lowest average heat flux was obtained at the S/d ratio of 10.

The effect of Re on the average heat flux distribution are shown in Fig. 11(b). It was observed that the average heat flux increased with increasing Re, following the variation of local heat flux distributions as shown in Fig. 9.

The effects of the S/d ratio on the average heat flux distribution are shown in Fig. 11(c). It was observed that in the region of $x/d \leqslant 10$, the average heat flux increased slightly with increasing S/d ratio when $S/d \leqslant 6$, while decreased relatively significantly as the S/d ratio was further increased to 10.

5. Conclusions

Experiments were carried out to investigate the heat transfer characteristics of a pair of laminar premixed butane/air circular flame jets, impinging on a flat plate. The impingement surface pressures exerted by the impinging flame jets were measured to assist in understanding the change in the jet flow. Effects of the S/d ratio, H/d ratio and Re on both the local and average heat fluxes were examined. The conclusions of the present study could be drawn as follows:

(1) The interference between the two jets increased with decreasing S/d ratio. For a small S/d ratio of 2.6, the two free flame jets coalesced into one enlarged single jet. For the S/d ratio of 6 and the largest S/d ratio of 10, this phenomenon did not occur. The stronger the interference between the jets, the greater would be the surface pressures in the between-jet area. This between-jet interference reduced the heat transfer rate in the interacting region at the small S/d ratio of 2.6, because of the occurrence of the second stagnation point at the midway between the two jets. It led to an anti-pressure gradient and the separation of the inner reaction layer from the impingement plate after the collision. Thus, the unburned butane/air mixture impinged directly on the plate and gave rise to a great decrease in heat flux at the midpoint where collision occurred between the two jets. On the other hand, this interference could increase the heat transfer rate at the S/d ratio of 6. This was because the interference-induced-turbulence enhanced the heat transfer coefficient.

(2) The interference between the two jets increased with decreasing H/d ratio. When $H/d = 2$, a second wall pressure peak occurred at the midpoint between the flame jets, which resulted in the downward flow of the wall jets after collision. The heat transfer increased with increasing H/d ratio due to the reduced interference between the two jets until $H/d = 6$. When the H/d ratio was further increased to 7, both the local heat flux and the average heat flux along the x-axis began to decrease because the high temperature inner reaction zone could no longer reach the impingement plate.

Acknowledgements

The authors wish to thank The Hong Kong Polytechnic University for financial support of the present study (project code: GV-323).

References

[1] R.N. Koopman, E.M. Sparrow, Local and average transfer coefficients due to an impinging row of jets, Int. J. Heat Mass Transfer 19 (1976) 673–683.

[2] B.R. Hollworth, R.D. Berry, Heat transfer from arrays of impinging jets with large jet-to-jet spacing, J. Heat Transfer 100 (1978) 352–357.

[3] L.W. Florschuetz, R.A. Berry, D.E. Metzger, Periodic stream-wise variations of heat transfer coefficients for inline and staggered arrays of circular jets with crossflow of spent air, J. Heat Transfer 102 (1980) 132–137.

[4] H. Laschefski, T. Cziesla, G. Biswas, N.K. Mitra, Numerical investigation of heat transfer by rows of rectangular impinging jets, Numer. Heat Transfer—Part A 30 (1996) 87–101.

[5] N.R. Saad, S. Polat, W.J.M. Douglas, Confined multiple impinging slot jets without crossflow effects, Int. J. Heat Fluid Flow 13 (1992) 2–14.

[6] R. Gardon, J.C. Akfirat, Heat transfer characteristics of impinging two-dimensional air jets, J. Heat Transfer 88 (1966) 101–108.

[7] R. Gardon, J. Cobonpue, Heat transfer between a flat plate and jets of air impinging on it, Int. Develop. Heat Transfer, Int. Heat Transfer Conf. 2 (1962) 454–460.

[8] P. Hrycak, Heat transfer from a row of impinging jets to concave cylindrical surfaces, Int. J. Heat Mass Transfer 24 (1980) 407–419.

[9] M. Korger, F. Krizek, Mass-transfer coefficient in impingement flow from slotted nozzles, Int. J. Heat Mass Transfer 9 (1966) 337–344.

[10] N.R. Saad, A.S. Mujumdar, W.J.M. Douglas, Heat transfer under multiple turbulent slot jets impinging on a flat plate, Drying'80 1 (1980) 422–430.

[11] S.H. Seyedein, M. Hasan, A.S. Mujumdar, Turbulent flow and heat transfer from confined multiple impinging slot jets, Numer. Heat Transfer—Part A 27 (1995) 35–51.

[12] A.H. Shiravi, A.S. Mujumdar, G.J. Kubes, Numerical study of heat transfer and fluid flow in multiple turbulent impinging jets, Drying Technol. 13 (1995) 1359–1375.

[13] X. Yan, N. Saniei, Measurements of local heat transfer coefficients from a flat plate to a pair of circular air impinging jets, Exp. Heat Transfer 9 (1996) 29–47.

[14] H. Martin, Heat and mass transfer between impinging gas jets and solid surfaces, Adv. Heat Transfer 13 (1977) 1–60.

[15] S. Polat, B. Huang, A.S. Mujumdar, W.J.M. Douglas, Numerical flow and heat transfer under impinging jets: a review, Ann. Rev. Numer. Fluid Mech. Heat Transfer 2 (1989) 157–197.

[16] R.J. Kind, K. Suthanthiran, The interaction of two opposing plane turbulent wall jets, AIAA paper 72-211, AIAA 10th Aerospace Sciences meeting, San Diego, CA, 1972.

[17] B.S. Stratford, The prediction of separation of the turbulent boundary layer, J. Fluid Mech. 5 (1959) 1–16.

[18] A.A. Townsend, The behavior of a turbulent boundary layer near separation, J. Fluid Mech. 12 (1961) 536–554.

[19] E. Baydar, Confined impinging air jet at low Reynolds numbers, Exp. Thermal Fluid Sci. 19 (1999) 27–33.

[20] A.M. Huber, Heat transfer with impinging gaseous jet systems, Ph.D. thesis, Purdue University, 1993.

[21] R.N. Koopman, Local and average transfer coefficients for multiple impinging jets, Ph.D. thesis, University of Minnesota, 1975.

[22] C. Carcasci, An experimental investigation on air impinging jets using visualization methods, Int. J. Thermal Sci. 38 (1999) 808–818.

[23] J.M.M. Barata, D.F.G. Durao, M.V. Heitor, Impingement of single and twin turbulent jets through a crossflow, AIAA J. 29 (1991) 595–602.

[24] J.M.M. Barata, D.F.G. Durao, M.V. Heitor, Velocity characteristics of multiple impinging jets through a crossflow, J. Fluids Eng. 114 (1992) 231–239.

[25] S.J. Slayzak, R. Viskanta, F.P. Incropera, Effects of interactions between adjoining rows of circular, free-surface jets on local heat transfer from the impingement surface, J. Heat Transfer 116 (1994) 88–95.

[26] D.R. Kotansky, L.W. Glaze, The effects of ground wall-jet characteristics on fountain up-wash flow formation and development, Report ONR-CR212-261-1F, 1980.

[27] E. Tanaka, The interference of two-dimensional parallel jets (first report, experiments on dual jet), Bull. JSME 13 (1970) 272–280.

[28] E. Tanaka, The interference of two-dimensional parallel jets (second reports, experiments on the combined flow of dual jet), Bull. ASME 17 (1974) 920–927.

[29] S. Mikhail, S.M. Morcos, M.M.M. Abou-Ellail, W.S. Ghaly, Numerical prediction of flow field and heat transfer from a row of laminar slot jets impinging on a flat plate, Heat Transfer 3 (1982) 377–382.

[30] N.T. Obot, T.A. Trabold, Impingement heat transfer within arrays of circular jets: Part 1—effects of minimum, intermediate, and complete crossflow for small and large spacings, J. Heat Transfer 109 (1987) 872–879.

[31] C.E. Baukal, B. Gebhart, Oxygen-enhanced/natural gas flame radiation, Int. J. Heat Mass Transfer 40 (1998) 2539–2547.

[32] J.M. Beer, N.A. Chigier, Impinging jet flames, Combust. Flame 12 (1968) 575–586.

[33] M. Fairweather, J.K. Kilham, A. Mohebi-Ashtiani, Stagnation point heat transfer from turbulent methane-air flames, Combust. Sci. Technol. 35 (1984) 225–238.

[34] G.K. Hargrave, M. Fairweather, J.K. Kilham, Forced convective heat transfer from premixed flames—part 1: flame structure, Int. J. Heat Fluid Flow 8 (1987) 55–63.

[35] K. Kataoka, Optimal nozzle-to-plate spacing for convective heat transfer in nonisothermal, variable-density impinging jets, Drying Technol. 3 (1985) 235–254.

[36] A. Milson, N.A. Chigier, Studies of methane and methane-air flames impinging on a cold plate, Combust. Flame 21 (1973) 295–305.

[37] J.R. Rigby, B.W. Webb, An experimental investigation of diffusion flame jet impingement heat transfer, Proceedings of the ASME/JSME Thermal Engineering Joint Conference, vol. 3, 1995, pp. 117–126.

[38] Th.H. Van der Meer, Heat transfer from impinging flame jets, Ph.D. thesis, Delft University of Technology, Netherland, 1987.

[39] G.K. Malikov, D.L. Lobanov, Y.K. Malikov, V.G. Lisienko, R. Viskanta, A.G. Fedorov, Experimental and numerical study of heat transfer in a flame jet impingement system, J. Inst. Energy 72 (1999) 2–9.

[40] J.W. Mohr, J. Seyed-Yagoobi, R.H. Page, Heat transfer characteristics of a radial jet reattachment flame, J. Heat Transfer 119 (1997) 258–264.
[41] J. Wu, J. Seyed-Yagoobi, R.H. Page, Heat transfer and combustion characteristics of an array of radial jet reattachment flames, Combust. Flame 125 (2001) 955–964.
[42] R. Viskanta, Heat transfer to impinging isothermal gas and flame jets, Exp. Thermal Fluid Sci. 6 (1993) 111–134.
[43] R. Viskanta, Convective and radiative flame jet impingement heat transfer, The 9th International Symposium on Transport Phenomena in Thermal-Fluids Engineering, 1996, pp. 46–60.
[44] L.L. Dong, C.S. Cheung, C.W. Leung, Heat transfer from an impinging premixed butane/air slot flame jet, Int. J. Heat Mass Transfer 45 (2002) 979–992.
[45] L.L. Dong, C.W. Leung, C.S. Cheung, Heat transfer of a row of three butane/air flame jets impinging on a flat plate, Int. J. Heat Mass Transfer 46 (2003) 113–125.
[46] S.J. Kline, F.A. McClintock, Describing uncertainties in single-sample experiments, Mech. Eng. 75 (1953) 3–8.
[47] K.R. Saripalli, Laser doppler velocimeter measurements in 3-D impinging twin-jet fountain flows, in: Turbulent Shear Flows, vol. 5, Sringer-Verlag, 1987, pp. 146–168.
[48] R.J. Goldstein, W.S. Seol, Heat transfer to a row of impinging circular air jets including the effect of entrainment, Int. J. Heat Mass Transfer 34 (1991) 2133–2147.
[49] R.J. Goldstein, J.F. Timmers, Visualization of heat transfer from arrays of impinging jets, Int. J. Heat Mass Transfer 25 (1982) 1857–1868.